Lifetime Analysis of Ferritic Steel Structures for High Temperature Fusion Applications

B.B. Glasgow and W.G. Wolfer

February 1985

UWFDM-615

Presented at the Sixth Topical Meeting on the Technology of Fusion Energy, San Francisco, CA, 3-7 March 1985; Fusion Tech. 8, (July 1985).

FUSION TECHNOLOGY INSTITUTE

UNIVERSITY OF WISCONSIN

MADISON WISCONSIN

"LEGAL NOTICE"

"This work was prepared by the University of Wisconsin as an account of work sponsored by the Electric Power Research Institute, Inc. ("EPRI"). Neither EPRI, members of EPRI, the University of Wisconsin, nor any person acting on behalf of either:

"a. Makes any warranty or representation, express or implied, with respect to the accuracy, completeness, or usefulness of the information contained in this report, or that the use of any information, apparatus, method, or process disclosed in this report may not infringe privately owned rights; or

"b. Assumes any liabilities with respect to the use of, or for damages resulting from the use of, any information, apparatus, method or process disclosed in this report."

Lifetime Analysis of Ferritic Steel Structures for High Temperature Fusion Applications

B.B. Glasgow and W.G. Wolfer

Fusion Technology Institute
University of Wisconsin
1500 Engineering Drive
Madison, WI 53706

http://fti.neep.wisc.edu

February 1985

UWFDM-615

Presented at the Sixth Topical Meeting on the Technology of Fusion Energy, San Francisco, CA, 3-7 March 1985; Fusion Tech. 8, (July 1985).

LIFETIME ANALYSIS OF FERRITIC STEEL STRUCTURES

FOR HIGH TEMPERATURE FUSION APPLICATIONS

B.B. Glasgow and W.G. Wolfer, Nuclear Engineering Department
University of Wisconsin-Madison, 1500 Johnson Drive
Madison, Wisconsin 53706
(608) 263-8142 or (608) 263-6818

ABSTRACT

Ferritic steels have been shown to swell much less than 316 austenitic stainless steel. For this reason ferritic steels are being considered for fusion reactor applications as an alternative to 316 austenitic stainless steel. A lifetime analysis based on crack propagation has been done for ferritic steel using typical first wall parameters. The results for ferritic steel are compared to results from a similar analysis done for 316 austenitic stainless steel. The comparison shows that ferritic steels have lower thermal stresses than 316 austenitic stainless steel by a factor of about 2. Because of the lower thermal stresses, the cyclic stresses resulting from the plasma-on/plasma-off cycles are reduced and the predicted fatigue crack growth rate is less for ferritic steels. The analysis predicts a lifetime more than 10 times longer for ferritic steel than for 316 austenitic stainless steel. The comparison clearly shows the great potential of ferritic steel over 316 austenitic stainless steel as a first wall material to achieve the high wall loading desired for future fusion reactors.

INTRODUCTION

Both experimental[1] and theoretical[2] work on 316 austenitic stainless steel show a long term swelling rate of about 1%/dpa. For ferritic steel, however, initial experimental work[1] shows a swelling rate of about 0.1%/dpa; theoretical work[2,3] predicts a maximum swelling rate of about 0.3%/dpa. Because of the much lower swelling rate of ferritic steels, these steels are being considered as an alternate material to 316 austenitic stainless steel. Another advantage of ferritic steels is their much reduced thermal stresses. Ferritic steel is a better thermal conductor than 316 austenitic stainless steel, and has a lower coefficient of thermal expansion. Because of these better thermophysical properties, the cyclic stresses which arise because of cyclic heat flux from the plasma (plasma-on/plasma-off cycles) are reduced. The reduction in cyclic stress is directly responsible for the improved fatigue crack growth performance of ferritic steel over 316 austenitic stainless steel.

Any lifetime analysis must consider the stress distribution through the structure as well as how the stresses will evolve with time due to stress relaxation and swelling. There have only been a handful of studies done for stress distribution evolution of fusion reactor high heat flux structures. Two of the most recent and most complete studies were done by Mattas[4] and Watson et al.[5] The results indicate that in modeling the stress evolution in a high heat flux fusion environment both creep relaxation and differential swelling must be included. The stress distribution model used in the analysis discussed herein is based on the model used by Watson et al. The model includes the effects of membrane loads, thermal and irradiation creep, differential swelling, and thermal expansion. The results of the stress distribution model are used as input into a crack propagation model. The end-of-life of the structure is assumed to occur when a preexisting crack propagates through the wall resulting in a breach of the pressure boundary. Early work done by Cramer et al.[6] identified crack growth as the life limiting failure mechanism in tokamak reactors.

The most complete work on crack propagation in fusion reactor first walls has been done by Watson et al.[5] Watson et al. modeled a 316 austenitic stainless steel tokamak reactor first wall. The results indicate that fatigue crack growth is the dominant crack growth mechanism. Fatigue crack growth causes an initially small crack to grow either completely through the wall in a slow manner or partially through the wall until the crack reaches a critical size for brittle fracture. Both modes result in failure; however, brittle fracture may be much more catastrophic in terms of damage to the fusion reactor itself and the present analysis distinguishes the two failure modes.

STRESS ANALYSIS

The first wall of a fusion reactor will be exposed to several adverse conditions. Not only will membrane loads and bending moments exist but there will be a high neutron flux, high temperatures and temperature gradients, differential swelling, and thermal and irradiation creep. All of the above mentioned conditions are included in the two dimensional stress distribution evolution model. Since most fusion first wall designs specify a thin walled structure because of the high heat flux, the stress state is assumed to be plane. Furthermore, in order to conservatively predict the magnitude of the stresses, a plate element constrained from bending but free to expand is assumed to represent the most critical part of the first wall. This generic element of the first wall structure is shown in Fig. 1.

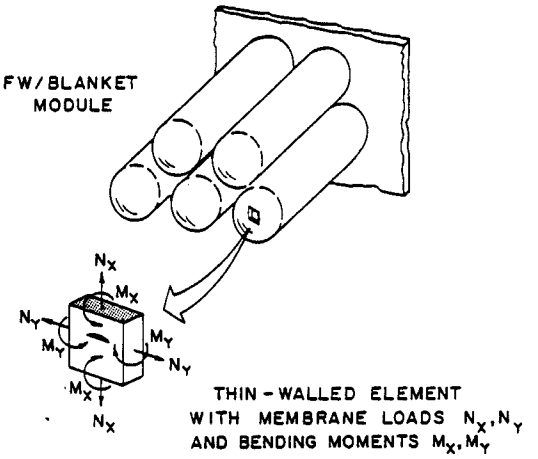

Fig. 1. Generic first wall plate element model from the tip of a blanket module.

For a plate element of thickness h free to bend and expand, one of the principal stresses is given by

$$\sigma_x(z) = \frac{N_x}{h} + \frac{12\,M_x z}{h^3} + \frac{E}{(1-\nu^2)h} \int_{-h/2}^{h/2} (e_x + \nu e_y)\,dz - \frac{E}{(1-\nu^2)}(e_x + \nu e_y) + \frac{12\,Ez}{(1-\nu^2)h^3} \int_{-h/2}^{h/2} (e_x + \nu e_y) z\,dz \quad (1)$$

where the first two terms represent the elastic stress due to membrane loads N_x and bending moments M_x. The last three terms are due to the inelastic strains, e_x and e_y, such as thermal expansion, swelling, and creep. E is Young's modulus and ν is Poisson's ratio. For a plate constrained from bending the above equation is reduced to

$$\sigma_x(z) = \frac{N_x}{h} + \frac{E}{(1-\nu^2)h} \int_{-h/2}^{h/2} (e_x + \nu e_y)dz - \frac{E}{(1-\nu^2)}(e_x + \nu e_y)\,. \quad (2)$$

The stress distribution through the plate can be followed with time by calculating how the inelastic strains develop with time.

Inelastic strains arise from three sources: (1) thermal strains, (2) creep strains, and (3) swelling strains. Thermal strains are due to thermal expansion of the structure when the plasma is on. The thermal strain is found from the expression $e_{th} = \alpha(T - T_o)$ where α is the coefficient of thermal expansion and T_o is the reference temperature. There is, however, another aspect of thermal strains and the interrelation between thermal strain and creep. Initially the only inelastic strain is the thermal strain resulting in compressive stress at the plasma surface and tensile stress at the coolant surface. Over time as the stresses begin to relax by creep, the plasma-on stresses are reduced in magnitude and, accordingly, the plasma-off stresses increase in magnitude eventually resulting in a small plasma-on stress but a large plasma-off stress. The plasma-off stress is now tensile on the plasma surface and compressive on the coolant surface. An example of the stress evolution for ferritic steel is shown in Fig. 2. The creep strain is calculated by numerically integrating the thermal and irradiation creep strain rates. Using the relationships proposed by Gelles et al.,[7] irradiation creep is taken as the sum of a radiation-induced creep and a swelling-induced creep as $\dot{e}_c^{irr} = B\sigma^n\phi + D\dot{S}\sigma$ where B, n, and D are constants, ϕ is the dose rate, and $\dot{S}$ is the swelling rate. Gelles et al. also propose a thermal creep rate of $\dot{e}_c^{th} = A/(1 - ABt)$ where A and B are functions of temperature and stress, and t is time.

For ferritic steel the stresses evolve as shown in Fig. 2; the swelling strains are negligible in this case compared to thermal and creep strains. However, if swelling strains cannot be ignored as in the case of 316 austenitic stainless steel, a different stress distribution evolves. As swelling strains build up compressive stresses for plasma-on conditions increase on the plasma side; likewise, equilibrating

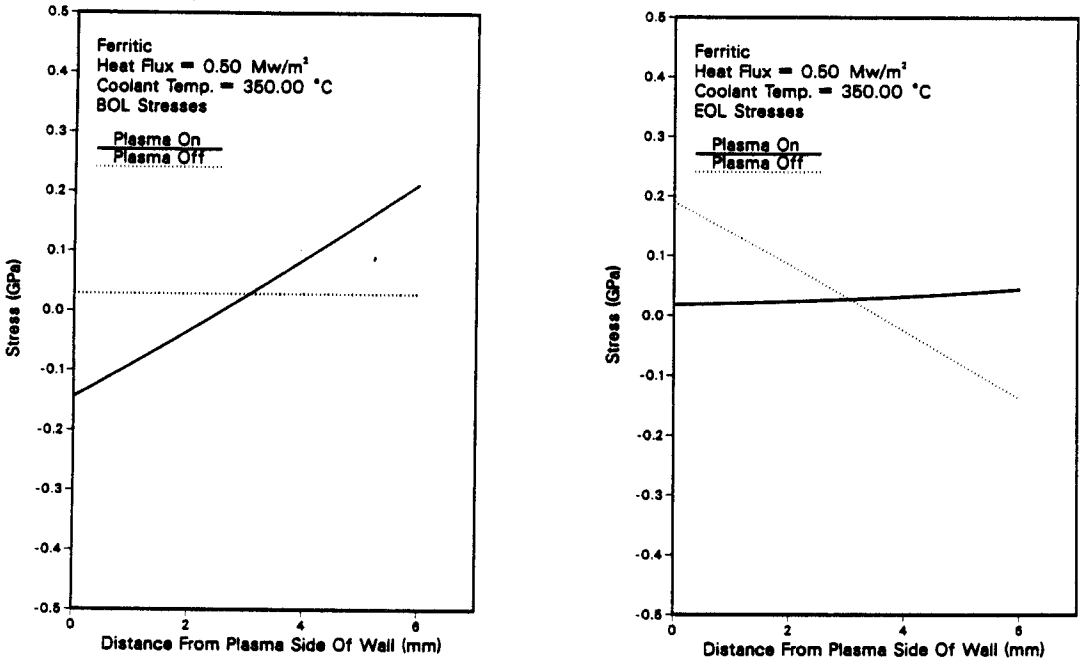

Fig. 2. First wall stress distribution at beginning-of-life and at end-of-life for 2-1/4 Cr-1 Mo.

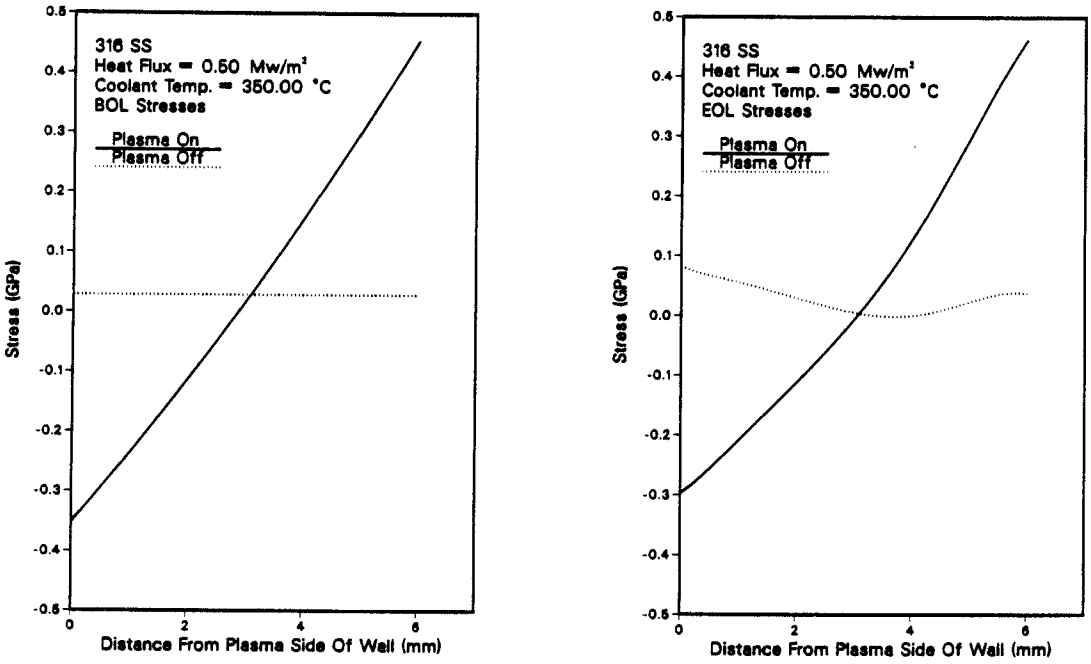

Fig. 3. First wall stress distribution at beginning-of-life and at end-of-life for 316 stainless steel.

tensile stresses increase on the coolant side. Now the interrelation between thermal, creep, and swelling strains results in a significantly different stress distribution later in life as is shown in Fig. 3. An additional interesting point on the stress evolution in 316 austenitic stainless steel is illustrated in Fig. 4. Up to 1 year of full power operation the stresses relax by creep. But, at approximately 1 year (the incubation period for the onset of swelling) the swelling strains begin and increase until a steady state is reached at about 3 years. This type of behavior is not predicted for ferritic steel because of the very low swelling rate and the extensive incubation period. The swelling rate for ferritic steel has been expressed in the empirical form

$$\dot{S} = R\phi\left[1 - \frac{1}{1 + e^{-\kappa}}\right] + De^{-\chi}\dot{\phi} \qquad (3)$$

by Gelles et al.[7] R and D are constants; κ and χ are functions of time, dose, and temperature.

FAILURE MODEL

A crack no matter how small could grow to sufficiently large size to compromise the integrity of the first wall. In fact, Cramer et al.[6] first identified crack growth as the limiting failure mechanism in 316 austenitic stainless steel tokamak first walls. End-of-life is presumed when a preexisting crack propagates through the plate causing a vacuum breach of the first wall. The mode of propagation can be either a slow crack propagation which will eventually cause a leak-through, or a rapid brittle fracture potentially causing catastrophic failure. In most cases a combination of the two modes occur. Early in life when the assumed crack is small, propagation is slow. However, as the crack increases in size the linear elastic fracture mechanics (LEFM) limit is reached and brittle fracture occurs. The present model allows the crack to grow independently in depth and width permitting elliptical cracks to be modeled.

Brittle fracture occurs whenever the stress intensity factor K exceeds the plane strain fracture toughness K_{Ic}. The plane strain fracture toughness is a material property allowed to change with the irradiation exposure. While the "plane stress" fracture is not generally regarded as a material property, it is known to be higher than the plane strain value. The model conservatively uses the plane strain value even through the stress distribution at the crack tip may be plane stress. For some metals (like body centered cubic ferritic steel) K_{Ic} is a strong function of temperature exhibiting a sharp drop in fracture toughness at the ductile to brittle transition temperature (DBTT). Other metals (like face centered cubic 316 austenitic stainless steel) do not exhibit a DBTT; but K_{Ic} is

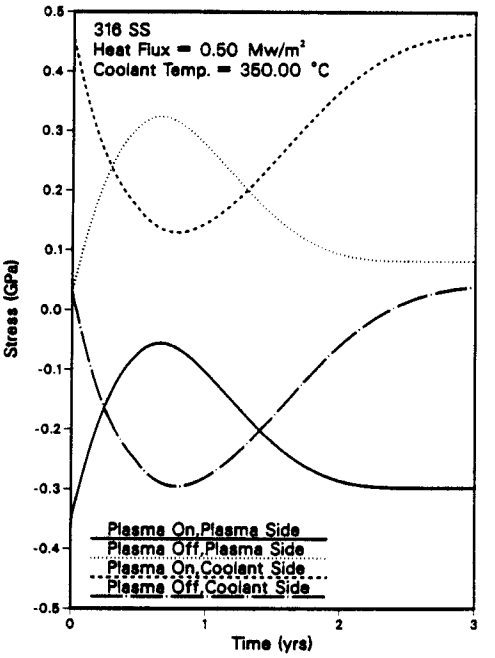

Fig. 4. First wall stresses as a function of time for 316 stainless steel.

still a mild function of temperature. Irradiation affects the fracture toughness of most metals by making the metals more brittle, thereby degrading the fracture toughness. Also for those metals exhibiting a DBTT, irradiation tends to move the DBTT to higher temperatures. To be conservative in modeling a ferritic steel first wall, the lower shelf fracture toughness for ferritic steel is used at all temperatures and a value of 30 MPa$\sqrt{m}$ is assumed. The fracture toughness of irradiated 316 austenitic stainless steel is similar to the lower shelf fracture toughness of irradiated ferritic steel and the same value is also assumed.

In the present analysis it is postulated that a semi-elliptical surface crack exists on either the plasma or the coolant side and that the element containing the crack is subject to a combination of membrane loads and bending loads. The bending loads arise from the various inelastic strains. The expression for the stress intensity factor[8] for this crack is

$$K = (M_m\sigma_m + M_b\sigma_b)\frac{1}{\sqrt{Q}}\sqrt{\pi a} \qquad (4)$$

where a is the crack depth, Q is the flaw shape factor, $M_{m,b}$ are the membrane and bending correction factors, and $\sigma_{m,b}$ are the membrane and bending stresses. In general, $M_{m,b}$ and Q are

functions of plate thickness, crack depth, and crack width. The model uses expressions for $M_{m,b}$ as given by Newman et al.[9]

Slow crack propagation proceeds by two mechanisms: (1) creep crack growth and (2) fatigue crack growth. Creep crack growth occurs at high temperatures when the crack tip is in a tensile stress field. The expression for creep crack growth rate for ferritic steel is of the form

$$\frac{da}{dt} = D_o e^{-Q/RT} (K_{max})^P \quad . \tag{5}$$

D_o, Q, R, and P are constants. Fatigue crack growth is the dominant crack growth mechanism for tokamaks unless the cyclic stress frequency were drastically reduced, as might be the case for a steady state device. The fatigue crack growth rate is modeled by the equation

$$\frac{da}{dN} = Cf \frac{[\Delta K^n - \Delta K_{th}^n]}{[1 - (\lambda f \Delta K / K_{Ic})^\lambda]} \tag{6}$$

where da/dN is the increase in crack dimensions with each cycle; C and n are constants, f is the ratio of Young's modulus at room temperature to the actual Young's modulus, ΔK is the cyclic stress intensity difference ($K_{max} - K_{min}$), ΔK_{th} is the threshold cyclic stress intensity below which no fatigue crack growth occurs, and $\lambda^{-1} = (1 - R)$ where $R = K_{min}/K_{max}$. Equation (6) above was used to correlate the experimental data of Suresh et al.[10] In particular, the threshold cyclic stress intensity ΔK_{th} data are those given in that reference. The threshold value is both a function of the R ratio (K_{min}/K_{max}) and the environment. Using the data for a dry hydrogen environment, the data can be correlated with the following relationship

$$\Delta K_{th} = \begin{cases} 3 + 10(0.25 - R), & \text{for } R < 0.25 \\ 3, & \text{for } R \geq 0.25 \end{cases} \tag{7}$$

which is shown is Fig. 5. The results for fatigue crack growth rate are shown in Fig. 6.

DISCUSSION

The method for the present lifetime analysis is illustrated in Fig. 7. The stress analysis is carried out with a code called TSTRESS; the results of TSTRESS are input into the crack propagation model WISECRACK. The input parameters for TSTRESS include wall thickness, heat flux, nuclear heating, coolant temperature, and inelastic strain constitutive laws. Besides the results of TSTRESS, the WISECRACK input includes

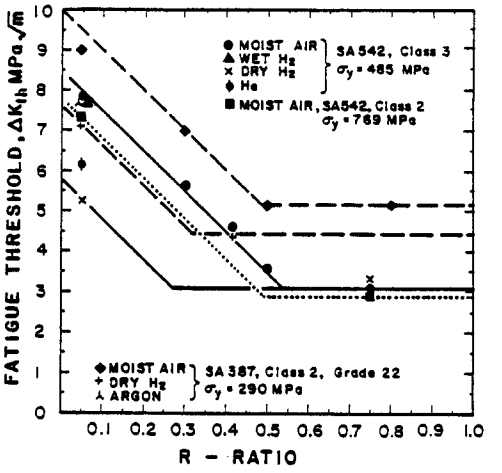

Fig. 5. Fatigue crack growth threshold versus R ratio showing the effect of environment.

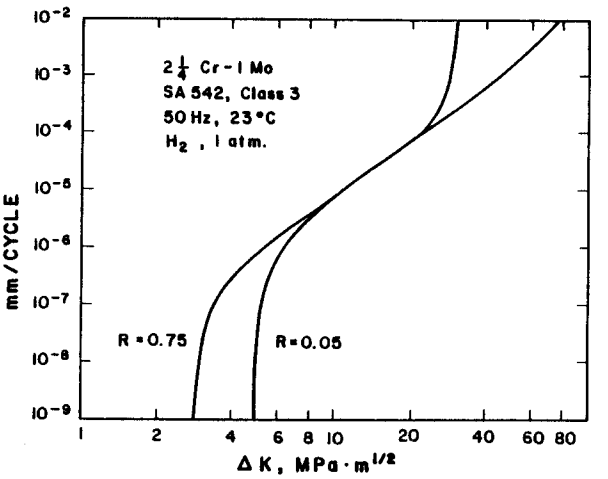

Fig. 6. Fatigue crack growth rates versus ΔK for 2-1/4 Cr-1 Mo.

flaw dimensions (depth and width), K_{Ic} as a function of temperature and dose, and the crack growth rates for fatigue and creep.

For the case of a first wall made of 316 austenitic stainless steel, Figs. 3 and 4 show the stress distribution and evolution. It can be seen in Fig. 4 that for times greater than about 3 years, the plasma side of the wall is subject mostly to tensile stresses. For long times then, it is the coolant side which seems most sensitive to crack propagation. If, however, failure occurs within less than 3 years, it is not obvious which side of the wall is most sensitive to crack growth. In the particular case shown here, it is predicted that a crack on the coolant side is more life limiting than a

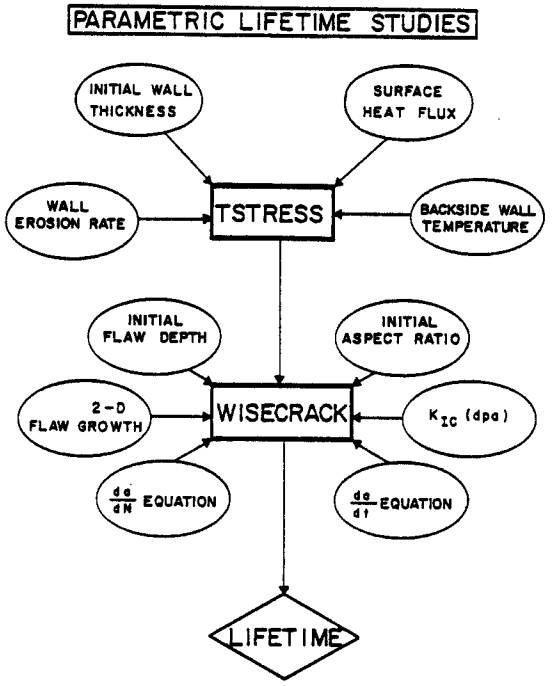

Fig. 7. Illustration of model used for lifetime calculations.

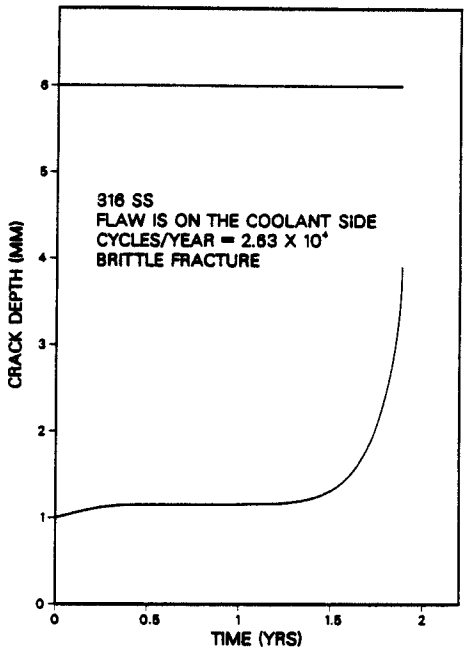

Fig. 8. Crack depth into first wall versus time for 316 stainless steel.

crack on the plasma side. Figure 8 shows the crack depth versus time for a crack on the coolant side. The length of time for a 1mm crack to propagate through the wall is approximately 2 years. The mode of failure is brittle fracture; the failure occurs when the crack dimensions are such that K exceeds K_{Ic}.

For ferritic steel, Fig. 2 shows the stress distribution at beginning-of-life and at end-of-life. The end-of-life distribution is, in fact, obtained in less than 2/10 of a year because of the rapid creep relaxation and negligible swelling. As illustrated in Fig. 2, the plasma side experiences the tensile cyclic stresses. The model predicts then that a crack on the plasma side is more critical than a crack on the coolant side. Under the same conditions as for 316 austenitic stainless steel, no failure is predicted for ferritic steel. In fact, the initial crack depth must be greater than about 3 times the initial crack depth for 316 austenitic stainless steel to get a failure within 30 years. Figure 9 illustrates the crack propagation for ferritic steel.

While the present lifetime analysis does not take all potential life limiting factors into account, it models in detail the crack propagation. Along with crack propagation, the effect of irradiation on K_{Ic} is also included, and an accurate evaluation of stress distribution and its evolution is accomplished. Based on this somewhat limited analysis, however, it is clear that ferritic steels have a great potential as a first wall material to achieve the long lifetimes desired for future fusion reactors.

ACKNOWLEDGEMENT

This work was sponsored by the Electric Power Research Institute under Contract No. RP-1597-2 with the University of Wisconsin-Madison.

REFERENCES

1. F.A. GARNER, ASTM-STP-870, to be published.

2. B.B. GLASGOW and W.G. WOLFER, ASTM-STP-870, to be published.

3. J.J. SNIEGOWSKI and W.G. WOLFER, Proceedings of the Topical Conference of Ferritic Alloys for Use in Nuclear Energy Technologies (Editors: J.W. Davis and D.J. Michel), page 579, The Metallurgical Society AIME, Warrendale (1984).

4. R.F. MATTAS, "Fusion Component Lifetime Analysis," ANL/FPP/TM-160 (1982).

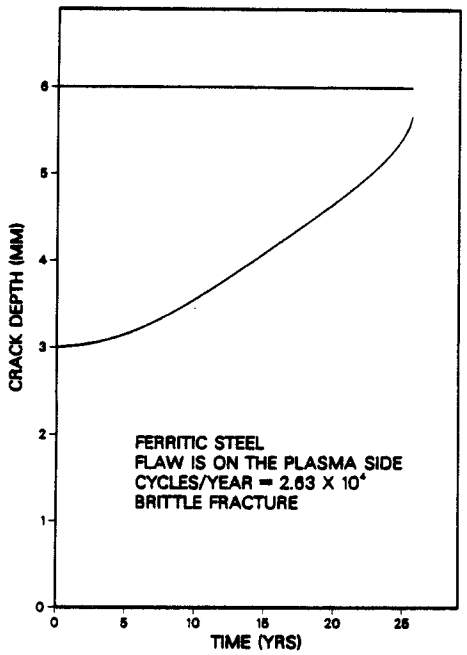

Fig. 9. Crack depth into first wall versus time for 2-1/4 Cr-1 Mo.

5. R.D. WATSON, R.R. PETERSON and W.G. WOLFER, "The Effect of Irradiation Creep, Swelling, Wall Erosion, and Embrittlement of the Fatigue Life of a Tokamak First Wall," J. of Nuclear Materials, 103, 97 (1981).

6. B.A. CRAMER, J.W. DAVIS, R.C. KINDER and D.A. BOWERS, "An Approach For Determining the Lifetime of a First Wall Structure in a Tokamak Reactor," CONF-760935-P4, Proceedings of the Second Topical Meeting on the Technology of Controlled Nuclear Fusion, Richland, WA (1976).

7. D.S. GELLES and R.J. PUIGH, "Evaluation of Ferritic Alloy Fe-2-1/4 Cr-1 Mo after Neutron Irradiation -- Irradiation Creep and Swelling," HEDL 7405 (1983).

8. ASME Boiler and Pressure Vessel Code, Section XI, Rules for Inservice Inspection of Nuclear Power Plant Components, Appendix A, Evaluation of Flaw Indicators (1977).

9. J.C. NEWMAN and I.S. RAJU, "Analysis of Surface Cracks in Finite Plates Under Tension or Bending Loads," NASA Technical Paper 1578 (1978).

10. S. SURESH, J. TOPLOSKY and R.O. RICHIE, "Environmentally Affected Near Threshold Fatigue Crack Growth in Steels," ASTM-STP-791 (1983).